IRIS AperTO

UNIVERSITÀ DEGLI STUDI DI TORINO

AperTO - Archivio Istituzionale Open Access dell'Università di Torino

Anharmonic Vibrational States of Solids from DFT Calculations. Part II: Implementation of the VSCF and VCI Methods

This is the author's manuscript

Original Citation:

Availability:

This version is available http://hdl.handle.net/2318/1710539 since 2019-08-26T14:02:31Z

Published version:

DOI:10.1021/acs.jctc.9b00294

Terms of use:

Open Access

Anyone can freely access the full text of works made available as "Open Access". Works made available under a Creative Commons license can be used according to the terms and conditions of said license. Use of all other works requires consent of the right holder (author or publisher) if not exempted from copyright protection by the applicable law.

(Article begins on next page)

16 November 2026

Anharmonic Vibrational States of Solids from DFT Calculations. Part II: Implementation of the VSCF and VCI Methods

Alessandro Erba,[1,*] Jefferson Maul,[1] Matteo Ferrabone,[1] Roberto Dovesi,[1] Michel Rérat,[2] and Philippe Carbonnière[2]

[1] *Dipartimento di Chimica, Universitá di Torino, via Giuria 5, 10125, Torino, Italy*
[2] *IPREM, Université de Pau et des Pays de l'Adour, IPREM-CAPT UMR CNRS 5254, Hélioparc Pau Pyrénées, 2 avenue du Président Angot, 64053 PAU CEDEX 9, Pau, France*

(Dated: April 26, 2019)

Two methods are implemented in the CRYSTAL program for the calculation of anharmonic vibrational states of solids: the vibrational self-consistent field (VSCF) and the vibrational configuration-interaction (VCI). While the former is a mean-field approach, where each vibrational mode interacts with the average potential of the others, the latter allows for an explicit and complete account of mode-mode correlation. Both schemes are based on the representation of the adiabatic potential energy surface (PES) discussed in Part I, where the PES is expanded in a Taylor's series so as to include up to cubic and quartic terms. The VSCF and VCI methods are formally presented and their numerical parameters discussed. In particular, the convergence of computed anharmonic vibrational states, within the VCI method, is investigated as a function of the truncation of the expansion of the nuclear wavefunction. The correctness and effectiveness of the implementation is discussed by comparing with available theoretical and experimental data on both molecular and periodic systems. The effect of the adopted basis set and exchange-correlation functional in the description of the PES on computed anharmonic vibrational states is also addressed.

I. INTRODUCTION

A reliable quantum-mechanical characterization of vibrational states of both molecular and solid systems is relevant to a correct description of a variety of properties: from their vibrational infrared and Raman spectroscopic fingerprint to their thermodynamic features, from their mechanical response to their non-linear optical properties, etc.[1] In the context of first principles quantum-mechanical simulations, when *ab initio* molecular dynamics (AIMD) is not used because of its high computational cost and its lack of vibration mode resolution, the description of the nuclear dynamics usually starts from the use of the harmonic approximation,[2–6] according to which the nuclear potential assumes a quadratic form with respect to atomic displacements and the atomic motion can be modeled in terms of a set of M independent quantum harmonic oscillators vibrating at frequencies ω_i with normal coordinates Q_i (with $i = 1, \cdots, M$). Harmonic frequencies and corresponding normal modes are nowadays routinely computed by most programs for molecular and periodic quantum-mechanical simulations.

Within the Born-Oppenheimer approximation, in the basis of normal coordinates, vibrational states are determined by solving the nuclear Schrödinger equation:

$$\mathcal{H}\Psi_s(\mathbf{Q}) = E_s\Psi_s(\mathbf{Q}) \,, \tag{1}$$

where $\Psi_s(\mathbf{Q})$ is the vibrational wavefunction of the s-th vibrational state and E_s the corresponding energy. By setting the rotational angular momentum to zero and by neglecting rotational coupling effects (note that while for solids there are no rotational contributions to the vibrational states, this assumption results in an approximation for molecules, where Coriolis coupling is neglected,[7–9] for instance), the vibrational Hamiltonian operator in Eq. (1) reduces to:

$$\mathcal{H} = \sum_{i=1}^{M} -\frac{1}{2}\frac{\partial^2}{\partial Q_i^2} + V(\mathbf{Q}) \,, \tag{2}$$

where $V(\mathbf{Q})$ is the Born-Oppenheimer potential energy surface (PES) in the basis of normal coordinates that we have discussed at length in Part I of the paper.[10] When higher order terms are included in the potential, the description of vibrational states becomes more problematic as vibrational modes couple together and therefore the differential Schrödinger equation above is no longer separable in the normal coordinates.

Different approaches (of increasing complexity and accuracy) can be used to solve it numerically. In particular, several methods have been developed to progressively take into account the correlation among vibration modes, through mode-mode couplings, which are formally analogous to the hierarchy of wavefunction-based methods in electronic structure theory.[11,12] The vibrational analog of the Hartree-Fock (HF) method is known as vibrational self-consistent field (VSCF) approach: a mean-field scheme where each vibrational degree of freedom interacts with an average potential over the other modes.[13–15] In analogy to the definition of dynamical electron correlation, the vibrational correlation among modes is defined as the difference between the exact vibrational states and VSCF ones. In electronic structure theory, the HF solution can be used as a starting point to improve the description of the electronic wavefunction, passing from a single-determinantal to a multi-determinantal representation by using either perturbative (MP2, MP4, etc.) or variational (CC, CI, etc.) approaches. In the vibration theory, starting from the ref-

erence VSCF state, the analog of the electronic Møller-Plesset perturbation theory is known as vibrational perturbation theory truncated at n-th order (VPTn),[16–18] the analog of the coupled-cluster family of methods is the vibrational coupled-cluster approach (VCC),[19,20] and the analog of the configuration-interaction methodology is the vibrational configuration-interaction (VCI), where mode-mode couplings are treated exactly (at least in the full-VCI limit).[21–30]

In this paper, we present the implementation in the CRYSTAL program[31,32] of the VSCF and VCI methods for both molecules and solids. In particular, this is the first implementation of VCI for periodic systems. The two methods are first illustrated from a formal point of view and are then used to describe the vibrational states of three simple molecular systems (water, methane and formaldehyde) and two solids (the MgH_2 magnesium hydride and the low-temperature proton-ordered phase of water ice, ice-XI). The effect of several parameters and different strategies on the convergence of VCI results with respect to the truncation of the VCI expansion of the nuclear wavefunction is critically addressed. The effect of the exchange-correlation functional of the DFT and the basis set used in the description of the PES on the computed anharmonic vibrational states of molecules and solids is explicitly discussed. Finally, comparisons with previously reported theoretical and experimental data are discussed.

II. METHODOLOGICAL ASPECTS

In this Section, we present into some detail the formalism of the VSCF and VCI methods for the calculation of anharmonic vibrational states of molecules and solids. As introduced in Part I,[10] we consider a system with M vibrational degrees of freedom (i.e. modes). Harmonic normal modes are represented in terms of normal coordinates $Q_1, Q_2, \cdots, Q_M$. We note that normal coordinates are perfectly defined even in cases where the harmonic approximation does not provide a satisfactory description of the nuclear dynamics of the system. Atomic units are used throughout the paper.

A. The Vibrational Self-Consistent Field (VSCF) Method

The vibrational self-consistent-field (VSCF) method is the vibrational analogue of the Hartree theory of electronic structure. At variance with electrons, vibrational modes are distinguishable so that the M-mode wavefunction of a given vibrational configuration $\mathbf{n}$ does not need to be antisymmetrized and can be written as a Hartree product of one-mode functions (modals):

$$\Phi^{\mathbf{n}}(Q_1, Q_2, \cdots, Q_M) \equiv \Phi^{\mathbf{n}}(\mathbf{Q}) = \prod_{i=1}^{M} \phi_i^{n_i}(Q_i) \ , \qquad (3)$$

where $\mathbf{n} = (n_1, n_2, \cdots, n_i, \cdots, n_M)$ is the vibrational configuration vector of the quantum numbers of the M one-mode functions. For each given vibrational state $\mathbf{n}$, the VSCF method consists in looking for the variationally best form of the corresponding M one-mode functions. This is achieved by requiring that the expectation value of the full Hamiltonian,

$$E^{\mathbf{n}} = \langle \Phi^{\mathbf{n}} | \mathcal{H} | \Phi^{\mathbf{n}} \rangle \qquad (4)$$

is stationary with respect to small variations in each of the modals with the orthonormality constraint on the modals:

$$\langle \phi_i^{n_i} | \phi_j^{m_j} \rangle = \delta_{ij} \delta_{nm} \ .$$

The Hamiltonian operator in Eq. (4) reads:

$$\mathcal{H} = \sum_{i=1}^{M} T_i + V(\mathbf{Q}) \ , \qquad (5)$$

where $T_i = -1/2(\partial^2/\partial Q_i^2)$ is the one-mode kinetic energy operator, and where $V(\mathbf{Q})$ is the Born-Oppenheimer potential energy surface (PES) that we have discussed into detail in Part I. In particular, we recall that the PES is expanded in a Taylor's series, centered at the equilibrium nuclear configuration, in terms of atomic displacements along normal coordinates. It proves useful to express the Hamiltonian in the following way:

$$\mathcal{H} = \sum_{i=1}^{M} h_i + V_c(\mathbf{Q}) \ , \qquad (6)$$

where h_i constitutes the separable part of the full Hamiltonian for the i-th mode:

$$h_i = -\frac{1}{2}\frac{\partial^2}{\partial Q_i^2} + \frac{1}{2}\omega_i^2 Q_i^2 + \frac{1}{6}\eta_{iii} Q_i^3 + \frac{1}{24}\eta_{iiii} Q_i^4 + \cdots \ , \qquad (7)$$

and $V_c(\mathbf{Q})$ is the coupling potential with all of those terms of the PES involving high-order (cubic, quartic, etc.) mixed energy derivatives with respect to two or more modes.

From the variational procedure mentioned above, for each vibrational state $\mathbf{n}$, the optimal VSCF modal functions can be obtained as eigenfunctions of the set of effective one-mode eigenvalue equations:

$$h_{\mathrm{eff},i}^{\mathbf{n}} \phi_i^{n_i}(Q_i) = \epsilon_i^{n_i} \phi_i^{n_i}(Q_i) \quad \text{for} \quad i = 1, \cdots, M \qquad (8)$$

where the one-mode effective Hamiltonian $h_{\mathrm{eff},i}^{\mathbf{n}}$ is given by:

$$\begin{aligned} h_{\mathrm{eff},i}^{\mathbf{n}} &= h_i + V_{\mathrm{eff},i}^{\mathbf{n}}(Q_i) \\ &= h_i + \left\langle \prod_{j\neq i}^{M} \phi_j^{n_j} \middle| V_c(\mathbf{Q}) \middle| \prod_{j\neq i}^{M} \phi_j^{n_j} \right\rangle \ . \end{aligned} \qquad (9)$$

The effective potential $V_{\mathrm{eff},i}^{\mathbf{n}}(Q_i)$ above is clearly a function of just Q_i because the coupling potential is averaged over the modal wavefunctions of the remaining

$M-1$ modes. These are simple one-dimensional eigenvalue equations, which, however, are coupled because the effective potential for any mode depends on the other modal eigenfunctions. These coupled equations can be solved with an iterative procedure starting from guess modal functions, used to evaluate the effective potentials. The eigenvalue equations are then solved and new modal eigenfunctions and eigenvalues obtained. The process goes on until convergence is reached.

The energy of the vibrational state $\mathbf{n}$ can then be obtained as the expectation value of the converged wavefunction, which yields:

$$E^{\mathbf{n}} = \langle \Phi^{\mathbf{n}} | \mathcal{H} | \Phi^{\mathbf{n}} \rangle = \sum_{i=1}^{M} \epsilon_i^{n_i} - (M-1) \langle \Phi^{\mathbf{n}} | V_c(\mathbf{Q}) | \Phi^{\mathbf{n}} \rangle \ .$$

In analogy with the Roothan linearization of the Hartree equations, each of the one-mode eigenvalue equations in Eq. (8) can be solved by matrix diagonalization by expressing the modals as a linear combination of basis functions:

$$\phi_i^{n_i}(Q_i) = \sum_{\nu=1}^{N_{\text{lev}}} C_{\nu,n_i} \psi_i^{\nu}(Q_i) \ . \tag{10}$$

In our implementation, $N_{\text{lev}} = 10$ (as this ensures a good description of all those vibrational states where each mode hosts few quanta of excitation) and the basis functions for the modals of the i-th mode are the eigenfunctions of the corresponding harmonic oscillator (HO):

$$\psi_i^{\nu}(Q_i) = \left(\frac{\sqrt{\omega_i}}{\sqrt{\pi} 2^{\nu} \nu!} \right)^{\frac{1}{2}} H_{\nu}(\xi_i) e^{-\frac{\xi_i^2}{2}} \ , \tag{11}$$

whose corresponding eigenvalues are:

$$\epsilon_{\nu,i} = \left(\frac{1}{2} + \nu \right) \omega_i \ ,$$

and where the $H_{\nu}(\xi_i)$ are Hermite polynomials of order ν in terms of the frequency-scaled coordinate $\xi_i = Q_i \sqrt{\omega_i}$. The eigenfunctions of each harmonic oscillator are orthonormal and therefore satisfy the following condition:

$$\langle \psi_i^{\nu} | \psi_i^{\mu} \rangle \equiv \int \psi_i^{\nu}(Q_i) \psi_i^{\mu}(Q_i) dQ_i = \delta_{\nu\mu} \ . \tag{12}$$

From the linearization in Eq. (10), the eigenvalue equation for each mode i in Eq. (8) can be expressed in the following matrix form:

$$\mathbf{H}^{\mathbf{n}}_{\text{eff},\mathbf{i}} \mathbf{C_i} = \mathbf{C_i} \mathbf{E_i} \ ,$$

where $\mathbf{E_i}$ is the diagonal matrix of the eigenvalues $\epsilon_i^{n_1}, \epsilon_i^{n_2}, \cdots, \epsilon_i^{n_N}$, $\mathbf{C_i}$ is the matrix of the eigenvectors, and $\mathbf{H}^{\mathbf{n}}_{\text{eff},\mathbf{i}}$ is the effective Hamiltonian matrix whose elements are:

$$\begin{aligned} \left(\mathbf{H}^{\mathbf{n}}_{\text{eff},\mathbf{i}} \right)_{\nu\mu} &= \int \psi_i^{\nu}(Q_i) h^{\mathbf{n}}_{\text{eff},i} \psi_i^{\mu}(Q_i) dQ_i \\ &\equiv \langle \psi_i^{\nu} | h^{\mathbf{n}}_{\text{eff},i} | \psi_i^{\mu} \rangle \ . \end{aligned} \tag{13}$$

1. Evaluation of the Effective Potential

Let us discuss how the effective Hamiltonian matrix elements in Eq. (13) can be evaluated. To do so, the calculation of the effective potential $V^{\mathbf{n}}_{\text{eff},i}(Q_i)$ in Eq. (9) has to be discussed. Having this purpose in mind, let us express the coupling potential $V_c(\mathbf{Q})$ (i.e. the sum of all mixed terms in the Taylor's expansion of the PES; see Part I) with the following compact notation:

$$V_c(\mathbf{Q}) = \sum_t \eta_t \prod_j Q_j^{p_{tj}} \ , \tag{14}$$

where each term t of the PES has a Taylor coefficient η_t and a product of normal coordinates of different modes to different powers, under the constraint that for cubic terms $\sum_j p_{tj} = 3$, for quartic terms $\sum_j p_{tj} = 4$, and so on. The effective potential for the i-th mode can thus be written as:

$$\begin{aligned} V^{\mathbf{n}}_{\text{eff},i}(Q_i) &= \left\langle \prod_{j \neq i} \phi_j^{n_j} \middle| V_c(\mathbf{Q}) \middle| \prod_{j \neq i} \phi_j^{n_j} \right\rangle \\ &= \sum_t \eta_t \left\langle \prod_{j \neq i} \phi_j^{n_j} \middle| \prod_j Q_j^{p_{tj}} \middle| \prod_{j \neq i} \phi_j^{n_j} \right\rangle \\ &= \sum_t \eta_t Q_i^{p_{ti}} \left\langle \prod_{j \neq i} \phi_j^{n_j} \middle| \prod_{j \neq i} Q_j^{p_{tj}} \middle| \prod_{j \neq i} \phi_j^{n_j} \right\rangle \\ &= \sum_t \eta_t Q_i^{p_{ti}} \prod_{j \neq i} \left\langle \phi_j^{n_j} \middle| Q_j^{p_{tj}} \middle| \phi_j^{n_j} \right\rangle \\ &= \sum_t \eta_t Q_i^{p_{ti}} \prod_{j \neq i} \sum_{\nu,\mu} C_{\nu,n_j} C_{\mu,n_j} \left\langle \psi_j^{\nu} \middle| Q_j^{p_{tj}} \middle| \psi_j^{\mu} \right\rangle \\ &= \sum_t X_t Q_i^{p_{ti}} \ , \end{aligned} \tag{15, 16}$$

where in the third passage the coordinate Q_i has been extracted from the integral as the integration is performed over the other $M-1$ coordinates and in the fifth passage the expansion of the modal functions in terms of corresponding harmonic eigenfunctions, as in Eq. (10), has been exploited. The mono-modal integrals in the right hand side of Eq. (15) can be calculated analytically as discussed below in Section II A 2.

In the end, from Eq. (16) we see that the effective potential $V^{\mathbf{n}}_{\text{eff},i}(Q_i)$ of the i-th mode is a sum of terms with coefficients X_t of powers of the normal coordinate Q_i. The effective Hamiltonian of Eq. (9) can then be written as:

$$h^{\mathbf{n}}_{\text{eff},i} = h_i + \sum_t X_t Q_i^{p_{ti}} \ ,$$

which, by recalling Eq. (7), can be given the following compact expression:

$$h^{\mathbf{n}}_{\text{eff},i} = -\frac{1}{2} \frac{\partial^2}{\partial Q_i^2} + \sum_r X_r Q_i^{p_{ri}} \ , \tag{17}$$

where the sum now runs over all the terms of the potential (diagonal and coupled). The effective Hamiltonian matrix elements in Eq. (13) can thus be expressed as:

$$\langle\psi_i^\nu|h^{\mathbf{n}}_{\text{eff},i}|\psi_i^\mu\rangle = \langle\psi_i^\nu|T_i|\psi_i^\mu\rangle + \sum_r X_r \langle\psi_i^\nu|Q_i^{p_{ri}}|\psi_i^\mu\rangle \ , \quad (18)$$

where T_i is the kinetic energy operator and where the mono-modal integrals in the last term are the same as the ones in Eq. (15) and can be computed analytically as discussed below.

2. Analytical Evaluation of Mono-modal Integrals

Let us discuss how the mono-modal integrals of Eq. (18) can be computed analytically. We start by considering the integrals related to the potential energy terms. Let us write them explicitly by recalling the expression in Eq. (11) for the eigenfunctions of the harmonic oscillator and by dropping the mode index i as here we only consider mono-mode integrals:

$$\langle\psi^\nu|Q^p|\psi^\mu\rangle = \frac{1}{\omega^{\frac{p+1}{2}}}\left(\frac{\sqrt{\omega}}{\sqrt{\pi}2^\nu\nu!}\right)^{1/2}\left(\frac{\sqrt{\omega}}{\sqrt{\pi}2^\mu\mu!}\right)^{1/2} \times \int_{-\infty}^{+\infty} e^{-\xi^2} H_\nu(\xi)\xi^p H_\mu(\xi) d\xi \ . \quad (19)$$

These integrals can be easily calculated by exploiting the following recursion property of Hermite polynomials:

$$H_{\nu+1}(\xi) = 2\xi H_\nu(\xi) - 2\nu H_{\nu-1}(\xi) \ , \quad (20)$$

and their ortho-normalization property:

$$\int_{-\infty}^{+\infty} H_\nu(\xi) H_\mu(\xi) e^{-\xi^2} d\xi = \sqrt{\pi}2^\nu\nu!\ \delta_{\nu\mu} \ . \quad (21)$$

As an example, we consider the case $p = 1$. From the recursion relation of Eq. (20) we get (here we drop the dependence on ξ of the Hermite polynomials for brevity):

$$\begin{aligned}\langle\psi^\nu|Q|\psi^\mu\rangle &= \frac{1}{\sqrt{\omega\pi}}\left(\frac{1}{2^\nu\nu!2^\mu\mu!}\right)^{1/2}\int_{-\infty}^{+\infty} e^{-\xi^2} H_\nu \xi H_\mu d\xi \\ &= \frac{1}{\sqrt{\omega\pi}}\left(\frac{1}{2^\nu\nu!2^\mu\mu!}\right)^{1/2}\int_{-\infty}^{+\infty} e^{-\xi^2}\left(\nu H_{\nu-1} + \frac{1}{2}H_{\nu+1}\right) H_\mu d\xi = \sqrt{\frac{\nu}{2\omega}}\,\delta_{\mu,\nu-1} + \sqrt{\frac{\nu+1}{2\omega}}\,\delta_{\mu,\nu+1} \ , \quad (22)\end{aligned}$$

where in the last step we have exploited the orthogonality condition of Eq. (21). It follows that only if $\mu = \nu \pm 1$ these integrals are not null:

$$\begin{aligned}\left\langle\psi^\nu\middle|Q\middle|\psi^{\nu-1}\right\rangle &= \sqrt{\frac{\nu}{2\omega}} \ ; \\ \left\langle\psi^\nu\middle|Q\middle|\psi^{\nu+1}\right\rangle &= \sqrt{\frac{\nu+1}{2\omega}} \ .\end{aligned}$$

By following the same strategy, analogous expressions can be derived for different values of the power p of Q. In particular, for $p = 2$ one gets that the only non-null integrals are:

$$\begin{aligned}\left\langle\psi^\nu\middle|Q^2\middle|\psi^{\nu-2}\right\rangle &= \frac{1}{2\omega}\sqrt{\nu(\nu-1)} \ ; \\ \left\langle\psi^\nu\middle|Q^2\middle|\psi^{\nu}\right\rangle &= \frac{1}{\omega}\left(\nu + \frac{1}{2}\right) \ ; \\ \left\langle\psi^\nu\middle|Q^2\middle|\psi^{\nu+2}\right\rangle &= \frac{1}{2\omega}\sqrt{(\nu+1)(\nu+2)} \ .\end{aligned}$$

Because of the virial theorem, these last integrals for the potential energy terms with $p = 2$ are particularly useful as they also describe the only non-null kinetic energy integrals in Eq. (18):

$$\begin{aligned}\left\langle\psi^\nu\middle|T\middle|\psi^{\nu-2}\right\rangle &\equiv -\frac{1}{2}\left\langle\psi^\nu\middle|Q^2\middle|\psi^{\nu-2}\right\rangle \ ; \\ \langle\psi^\nu|T|\psi^{\nu}\rangle &\equiv \frac{1}{2}\left\langle\psi^\nu\middle|Q^2\middle|\psi^{\nu}\right\rangle \ ; \\ \left\langle\psi^\nu\middle|T\middle|\psi^{\nu+2}\right\rangle &\equiv -\frac{1}{2}\left\langle\psi^\nu\middle|Q^2\middle|\psi^{\nu+2}\right\rangle \ .\end{aligned}$$

B. The Vibrational Configuration Interaction (VCI) Method

In analogy with the CI approach in electronic structure theory, in the VCI method, the wave-function of each vibrational state s is written as a linear combination of M-mode wave-functions of different vibrational configurations in the form of Hartree products of modals as in Eq. (3):

$$\Psi_s(\mathbf{Q}) = \sum_{n=1}^{N_{\text{conf}}} A_{n,s}\Phi^{\mathbf{n}}(\mathbf{Q}) \ , \quad (23)$$

where the sum runs over N_{conf} configurations, each characterized by a vibrational configuration vector $\mathbf{n}$ of the quantum numbers of the M one-mode functions. We are going to discuss later how the N_{conf} configurations are selected (i.e. how the CI expansion is truncated). For each

vibrational state s, the corresponding VCI wave-function and energy are obtained by solving the corresponding Schrödinger equation:

$$\mathcal{H}\Psi_s = E_s\Psi_s \ . \tag{24}$$

The VCI method can be expressed in matrix form as follows:

$$\mathbf{HA} = \mathbf{AE} \ , \tag{25}$$

where $\mathbf{A}$ is the squared matrix containing, column-wise, the coefficients $A_{n,s}$ of the eigenvectors, $\mathbf{E}$ is the diagonal matrix of the eigenvalues and $\mathbf{H}$ is the VCI Hamiltonian matrix (of size $N_{\rm conf} \times N_{\rm conf}$), whose elements are:

$$H_{m,n} = \langle \Phi^{\mathbf{m}} | \mathcal{H} | \Phi^{\mathbf{n}} \rangle \ . \tag{26}$$

The VCI method therefore reduces to the construction and diagonalization of the VCI Hamiltonian matrix from which all vibrational states are simultaneously determined. Let us now discuss how the VCI Hamiltonian matrix is built. By expressing the Hamiltonian operator as in Eq. (6), we have:

$$H_{m,n} = \left\langle \Phi^{\mathbf{m}} \left| \sum_i h_i \right| \Phi^{\mathbf{n}} \right\rangle + \langle \Phi^{\mathbf{m}} | V_c | \Phi^{\mathbf{n}} \rangle \ . \tag{27}$$

Let us analyze the two terms in the rhs of the expression above separately. By recalling the expansion in Eq. (3) of the vibrational configuration wave-functions in terms of modals, the first term becomes:

$$\begin{aligned} \left\langle \Phi^{\mathbf{m}} \left| \sum_i h_i \right| \Phi^{\mathbf{n}} \right\rangle &= \left\langle \prod_i \phi_i^{m_i} \left| \sum_i h_i \right| \prod_i \phi_i^{n_i} \right\rangle \\ &= \sum_i \left\langle \prod_i \phi_i^{m_i} \left| h_i \right| \prod_i \phi_i^{n_i} \right\rangle \\ &= \sum_i \langle \phi_i^{m_i} | \, h_i \, | \phi_i^{n_i} \rangle \prod_{j \neq i} \langle \phi_j^{m_j} | \phi_j^{n_j} \rangle \end{aligned} \tag{28}$$

By recalling the expression (14) for the coupling potential $V_c(\mathbf{Q})$, the second term on the rhs of Eq. (27) can be written as:

$$\begin{aligned} \langle \Phi^{\mathbf{m}} | V_c | \, \Phi^{\mathbf{n}} \rangle &= \left\langle \prod_i \phi_i^{m_i} \left| \sum_t \eta_t \prod_i Q_i^{p_{ti}} \right| \prod_i \phi_i^{n_i} \right\rangle \\ &= \sum_t \eta_t \prod_{i \, (p_{ti} \neq 0)} \langle \phi_i^{m_i} | Q_i^{p_{ti}} | \, \phi_i^{n_i} \rangle \prod_{j \, (p_{tj} = 0)} \langle \phi_j^{m_j} | \phi_j^{n_j} \rangle \end{aligned} \tag{29}$$

where in the last expression, for each term t of the coupling potential, the first product runs over those modes i whose powers p_{ti} differ from zero, and the second product runs over those modes j whose powers p_{tj} are zero.

Different choices are possible for the functions used to describe the modals $\phi_i^{n_i}$. The convergence of the computed vibrational states with respect to the number of configurations $N_{\rm conf}$ used in the CI expansion of the wave-function in Eq. (23) depends on this choice. This aspect of the VCI method will be illustrated into detail in Section IV. In this respect, the two most common choices (both ensuring the orthogonality of the basis functions) are the following:

1. Modals are taken to coincide with the corresponding HO wave-functions given in Eq. (11):

$$\phi_i^{n_i}(Q_i) = \psi_i^{\nu=n_i}(Q_i) \ . \tag{30}$$

   The resulting approach is often referred to as VCI@HO.

2. Modals are taken to coincide with the solutions of a previous VSCF calculation for a reference configuration and are therefore expressed as a linear combination of HO wave-functions as in Eq. (10):

$$\phi_i^{n_i}(Q_i) = \sum_{\nu=1}^{N_{\rm lev}} C_{\nu,n_i} \psi_i^{\nu}(Q_i) \ , \tag{31}$$

   where the coefficients C_{ν,n_i} are those obtained from a converged VSCF calculation on the reference configuration (typically chosen to be the ground state configuration). The resulting approach is often referred to as VCI@VSCF.

Within the VCI@HO approach, the integrals in Eqs. (28) and (29) reduce to:

$$\langle \phi_i^{m_i} | \, h_i \, | \phi_i^{n_i} \rangle \equiv \langle \psi_i^{m_i} | \, h_i \, | \psi_i^{n_i} \rangle \ ; \tag{32}$$

$$\langle \phi_i^{m_i} | Q_i^{p_{ti}} | \, \phi_i^{n_i} \rangle \equiv \langle \psi_i^{m_i} | Q_i^{p_{ti}} | \, \psi_i^{n_i} \rangle \ ; \tag{33}$$

$$\langle \phi_j^{m_j} | \phi_j^{n_j} \rangle \equiv \langle \psi_j^{m_j} | \psi_j^{n_j} \rangle = \delta_{m_j,n_j} \ , \tag{34}$$

where the overlap integrals over HO functions in Eq. (34) are Kronecker's delta from the orthogonality condition in Eq. (12), and where the mono-modal integrals in Eqs. (32) and (33) can be computed by following the procedure described in Section II A 2.

In the VCI@VSCF approach, the integrals in Eqs. (28) and (29) are evaluated as follows:

$$\langle \phi_i^{m_i} | \, h_i \, | \phi_i^{n_i} \rangle \equiv \sum_{\nu,\mu=1}^{N_{\rm lev}} C_{\mu,m_i} C_{\nu,n_i} \langle \psi_i^{\mu} | \, h_i \, | \psi_i^{\nu} \rangle \ ; \tag{35}$$

$$\langle \phi_i^{m_i} | Q_i^{p_{ti}} | \, \phi_i^{n_i} \rangle \equiv \sum_{\nu,\mu=1}^{N_{\rm lev}} C_{\mu,m_i} C_{\nu,n_i} \langle \psi_i^{\mu} | Q_i^{p_{ti}} | \, \psi_i^{\nu} \rangle \ ; \tag{36}$$

$$\langle \phi_j^{m_j} | \phi_j^{n_j} \rangle \equiv \sum_{\nu,\mu=1}^{N_{\rm lev}} C_{\mu,m_j} C_{\nu,n_j} \underbrace{\langle \psi_j^{\mu} | \psi_j^{\nu} \rangle}_{\delta_{\mu,\nu}} = \sum_{\nu=1}^{N_{\rm lev}} C_{\nu,m_j} C_{\nu,n_j} \ , \tag{37}$$

where the mono-modal integrals on the rhs of Eqs. (35) and (36) are the same needed in the VCI@HO approach and are computed as discussed in Section II A 2, and where the overlap integrals in Eq. (37) reduce to sums of products of appropriate VSCF coefficients.

1. The Truncation of the CI Expansion

The VCI method relies on the expansion of the wavefunction of each vibrational state in terms of N_{conf} Hartree product functions describing different vibrational configurations, as introduced in Eq. (23). The number N_{conf} of functions used in the VCI expansion is of critical importance with regard to both the accuracy and computational cost of the method. Indeed, the larger N_{conf} the better the description of the vibrational state but also the larger the size of the VCI Hamiltonian matrix in Eq. (27) to be diagonalized. In particular, this latter aspect is the main limiting factor to the application of standard VCI to the study of those systems where more than just a few vibration modes need to be coupled.

Therefore, it is crucial to devise effective schemes to reduce as much as possible the configurational space used in the VCI expansion. We are going to introduce two such schemes below, and to illustrate their effectiveness in reducing N_{conf}. Let us recall that each vibrational configuration used in the VCI expansion is characterized by a vibrational configuration vector $\mathbf{n} = (n_1, n_2, \cdots, n_i, \cdots, n_M)$, where the n_i are the vibrational quantum numbers of each of the M modes of the system. The following strategies can be used:

1. The first strategy for the truncation of the VCI expansion consists in including only those vibrational configurations where there are a maximum of N_{quanta} excitation quanta involved. Formally, we can express this strategy as follows to say that only those configurations satisfying the next condition are included in the expansion:

$$\sum_{i=1}^{M} n_i \leq N_{\text{quanta}} \; ; \tag{38}$$

2. A second strategy that we use to truncate the VCI expansion consists in setting a maximum number of modes N_{modes} that can be simultaneously excited in a given configuration. In other words, only those vibrational configurations where there are a maximum of N_{modes} with $n_i \neq 0$ are used.

The effect of these two schemes on the truncation of the VCI expansion is documented in Figure 1 for three values of M (i.e. of the number of vibration modes of the system). The figure reports the number of vibrational configurations used, N_{conf}, as a function of the two criteria for truncation introduced above: N_{quanta} and N_{modes}. It is seen that, while the number of configurations remains very low (never exceeding 120 in the explored range) for $M = 3$ (such as in molecular water), N_{conf} can already become quite large for $M = 9$ (such as in molecular methane) depending on the truncation of the expansion. Indeed, in this case, $N_{\text{quanta}} = 7$ and $N_{\text{modes}} = 5$ imply $N_{\text{conf}} > 10000$. For $M = 12$, the number of configurations increases further and, for

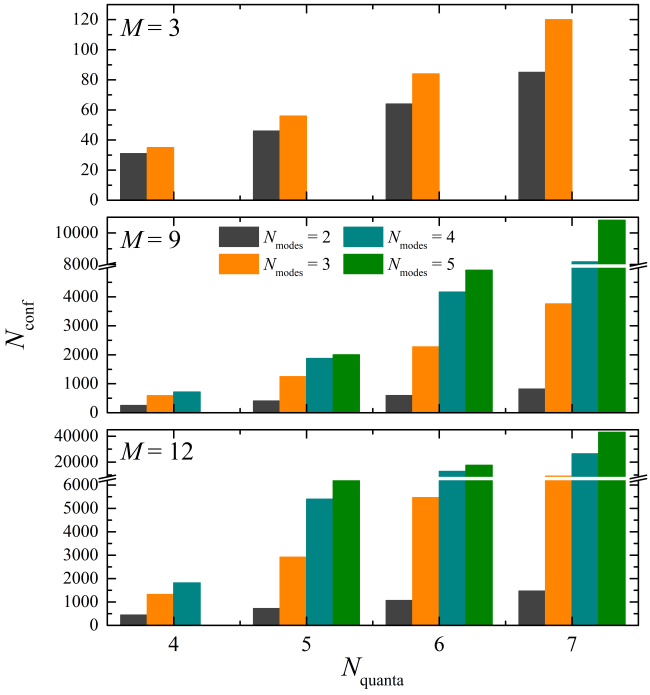


FIG. 1. Number of vibrational configurations N_{conf} used in the VCI expansion of Eq. (23) as a function of the two criteria of truncation introduced in Section II B 1: N_{quanta} and N_{modes}. The three panels correspond to three different values for M (i.e. for the total number of vibration modes).

$N_{\text{quanta}} = 7$ and $N_{\text{modes}} = 4$, gets to $N_{\text{conf}} > 20000$, which leads to a VCI Hamiltonian matrix that becomes problematic to be stored in memory and diagonalized.

Figure 1 clearly shows how crucial it is to truncate the VCI expansion according to relatively low values of the two criteria N_{quanta} and N_{modes}. We are going to discuss the explicit convergence of VCI vibrational states as a function of N_{quanta} in Section IV. As regards N_{modes}, let us anticipate that, when working in terms of 2M4T or 3M4T representations of the PES, the VCI description is converged for $N_{\text{modes}} = 3$ and $N_{\text{modes}} = 4$, respectively.

Apart from the aforementioned ways of truncating the VCI expansion, we also anticipate that expressing the modals in terms of functions obtained from a previous VSCF calculation (as done in the VCI@VSCF approach) allows to significantly reduce the size of the configurational space compared to the expansion of modals in terms of HO functions (as done in the VCI@HO approach). We are going to illustrate into detail this latter aspect in Section IV.

III. COMPUTATIONAL DETAILS

All calculations are performed with a developmental version of the CRYSTAL17 program, where the methodologies formally presented in Section II have been implemented.[31] Five systems are considered: three

molecules (water, H_2O, methane, CH_4, and formaldehyde, CH_2O) and two solids (the MgH_2 magnesium hydride and the low-temperature proton-ordered phase of water ice, Ice-XI). Apart from the formaldehyde molecule, the other systems are the same studied in Part I and therefore we refer to it for the description of the adopted basis sets and computational parameters.[10] For formaldehyde, the same 6-31G* basis set used for the other two molecules is adopted. We recall that, while all vibration modes are considered for the three molecular systems (i.e. $M = 3$ for water, $M = 6$ for formaldehyde, and $M = 9$ for methane in the construction of the PES and in the VSCF and VCI calculation of the anharmonic vibrational states), a subset of modes is used for the two solids, selected so as to span the whole spectrum of lattice vibrations. In particular, for MgH_2, ten vibration modes ($M = 10$) are considered (the smallest having a harmonic vibration frequency of 210 cm^{-1} and the largest of 1295 cm^{-1}), and for Ice-XI, twelve modes ($M = 12$) are selected (the smallest having a harmonic vibration frequency of 274 cm^{-1} and the largest of 3226 cm^{-1}).

In order to check the effect of the adopted basis set on the description of the vibrational anharmonicity, we have repeated all calculations for the three molecules with an augmented correlation-consistent triple-zeta basis set: aug-cc-pvtz.[33,34] We have also repeated all calculations for Ice-XI by using a triple-zeta basis set.[35] When not explicitly said otherwise, all calculations are performed by using the hybrid B3LYP functional of the DFT.[36] We also investigate the effect of the adopted Hamiltonian on the description of the anharmonicity of the systems by using the Hartree-Fock (HF) method and different functionals of the DFT (namely, PBE[37] and PBE0[38]).

The effect of those computational parameters that are specific to the adopted anharmonic methodologies illustrated in Section II is explicitly addressed in Section IV.

IV. RESULTS AND DISCUSSION

Here we discuss several aspects of the methodologies illustrated in Section II for the description of anharmonic vibration states in molecules and solids: i) the convergence of the computed vibrational states within the VCI method as a function of the truncation of its expansion; ii) the correctness of the current implementation of VCI by comparison with previous molecular implementations; iii) the effect of the quantum-mechanical methodology and basis set used in the calculation of the potential on the description of the vibrational anharmonicity of molecular and extended systems; iv) the comparison between the VSCF and VCI description of anharmonicity; v) the comparison between computed anharmonic states and experimental data.

We start by discussing the convergence of VCI states as a function of the truncation of the VCI expansion in Eq. (23) according to the criteria introduced in Section

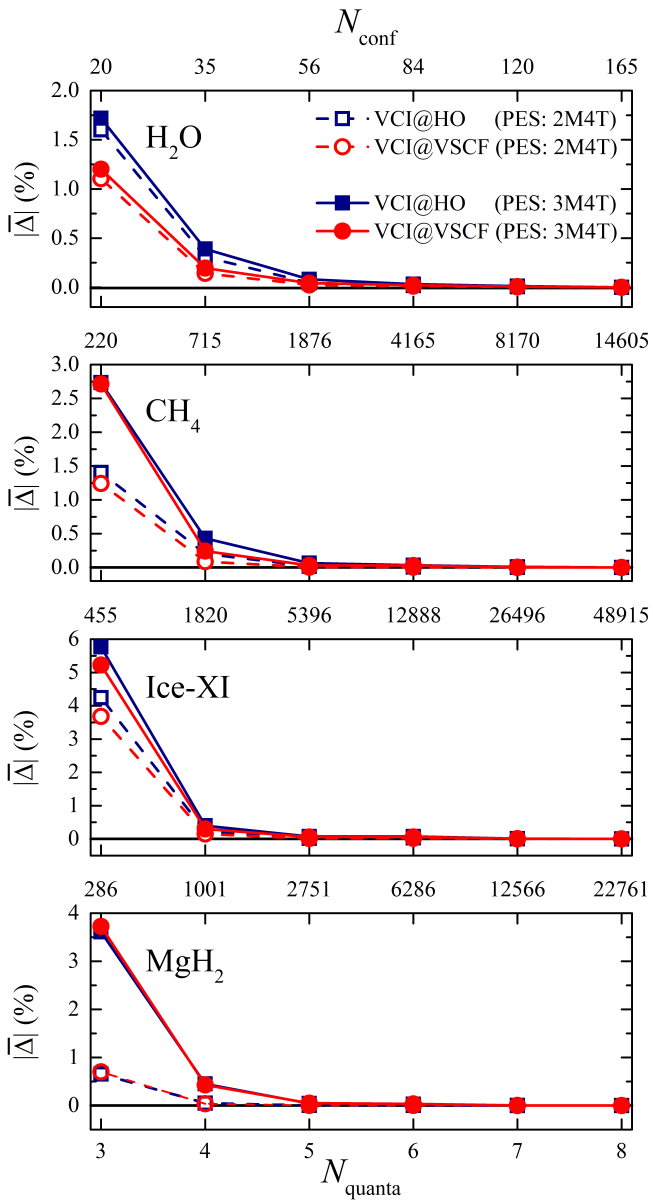


FIG. 2. Convergence of fundamental transition frequencies ($n_i = 0 \rightarrow 1$) as a function of the truncation of the VCI expansion. The four panels correspond to four different systems (from top: water molecule, methane molecule, solid Ice-XI, solid MgH_2). See text for an exact definition of all reported quantities.

II B 1. Several factors affecting the VCI convergence are explicitly discussed: i) the use of modals from a previous VSCF reference calculation versus the use of harmonic oscillator eigenfunctions as modals (i.e. VCI@VSCF versus VCI@HO); ii) the inclusion of up to two-mode or three-mode terms in the potential (i.e. a 2M4T versus a 3M4T description of the PES, as discussed in Part I); iii) the nature of the vibrational state relative to the vibrational ground state (fundamental transition involving one quantum of excitation, first-overtone involving two quanta of

excitation, second-overtone involving three quanta of excitation, combination bands, etc.).

Figure 2 shows the convergence with respect to the truncation of the VCI expansion of fundamental transitions of the type $n_i = 0 \rightarrow 1$ (i.e. of the vibrational ground state and of those vibrational states characterized by a single quantum of excitation) for the M considered modes of four systems: the water and methane molecules and the Ice-XI and MgH_2 crystals. The VCI expansion is truncated according to the two quantities $N_{\rm quanta}$ and $N_{\rm modes}$ introduced in Section II B 1. Here, $N_{\rm modes}$ is always set to 3 when the 2M4T representation of the potential is used and to 4 when the 3M4T representation is adopted, while the effect of $N_{\rm quanta}$ on the computed states is explicitly reported in the figure. The total number of configurations $N_{\rm conf}$ included in the VCI expansion as a function of $N_{\rm quanta}$ (for $N_{\rm modes} = 4$) is also given on the top of each panel. This latter quantity corresponds to the size of the VCI Hamiltonian matrix that needs to be diagonalized. We note in passing that for those systems (such as water and Ice-XI) that belong to Abelian symmetry point groups, we factorize the VCI matrix into diagonal sub-blocks specific to distinct irreducible representations (the exploitation of point-symmetry in the treatment of anharmonic states of molecules and solids in our implementation will be discussed into detail in a forthcoming paper). For each line of Figure 2, the quantity reported is the mean absolute deviation (in %) of the fundamental transition frequencies ω_i with respect to fully converged ones (i.e. those obtained for $N_{\rm quanta} = 8$):

$$|\overline{\Delta}|(\%) = \frac{1}{M}\sum_{i=1}^{M} \frac{\left|\omega_i^{N_{\rm quanta}} - \omega_i^{N_{\rm quanta}=8}\right|}{\left|\omega_i^{N_{\rm quanta}=8}\right|} \times 100\ . \quad (39)$$

In each panel of the figure (i.e. for each considered system), we report four data-sets: empty symbols refer to a 2M4T representation of the potential while filled symbols to a 3M4T representation; red symbols correspond to data obtained from the VCI@VSCF approach while blue symbols to data obtained from the VCI@HO method. Several considerations can be made: i) the computed anharmonic fundamental transitions of all systems, molecular and crystalline, show a very regular convergence as a function of the truncation of the VCI expansion; ii) the singly-excited vibrational states are still far from being converged when the expansion is truncated according to $N_{\rm quanta} = 3$ (with mean deviations as large as 6% for Ice-XI) while the convergence is much improved for $N_{\rm quanta} = 4$ with deviations dropping below 0.5% in all cases; iii) in all cases, the inclusion of three-mode terms in the PES (i.e. force constants of type η_{ijk} and η_{iijk} discussed in Part I) results in larger deviations at small $N_{\rm quanta}$ and thus in a slightly slower convergence with respect to a two-mode potential (compare filled to empty symbols in the figure, particularly so for methane and MgH_2); iv) smaller deviations and thus a slightly faster convergence of the computed anharmonic states are obtained when using the VCI@VSCF approach compared to the VCI@HO approach (see red versus blue symbols).

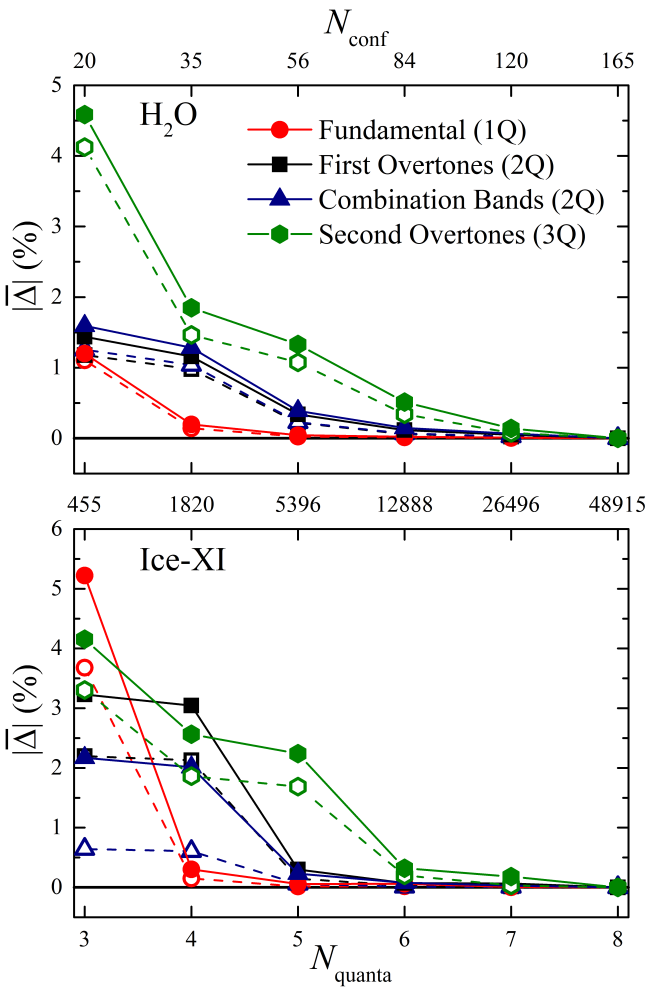


FIG. 3. Convergence as a function of the truncation of the VCI expansion of fundamental transitions (involving one quantum of excitation, 1Q), first and second overtones (involving two and three quanta of excitation, 2Q and 3Q, respectively), and combination bands with 2Q. The two panels correspond to water molecule (top) and solid Ice-XI (bottom). Reported quantities as in Figure 2. All values are computed with the VCI@VSCF approach. Filled and empty symbols correspond to 3M4T and 2M4T representations of the PES, respectively.

So far, we have discussed the convergence, with respect to the truncation of the VCI expansion, of vibrational states characterized by either zero quanta of excitation (i.e. the vibrational ground state) or a single quantum of excitation, 1Q. Now, we address the convergence of vibrational states characterized by a higher number of excitation quanta: first overtones ($n_i = 0 \rightarrow 2$), two-quanta combination states ($n_i = 0 \rightarrow 1$ and simultaneously $n_j = 0 \rightarrow 1$), and second overtones ($n_i = 0 \rightarrow 3$). The convergence of these states is illustrated in the two panels of Figure 3 for the water molecule (upper panel) and solid Ice-XI (lower panel). The structure of Fig-

TABLE I. Effect of basis set and Hamiltonian on computed harmonic and anharmonic vibration frequencies (in cm^{-1}) of water, methane and formaldehyde. Two basis sets are used: a 6-31G* (BSa) and an aug-cc-pvtz (BSb). The Hartree-Fock (HF) method is used along with three exchange-correlation functionals of the DFT: PBE, PBE0 and B3LYP. When the effect of the Hamiltonian is investigated, the BSa is adopted. For each system, the harmonic (HA) values are reported along with the anharmonic correction (Δ) obtained with the VCI@VSCF method on a 3M4T representation of the PES.

	B3LYP				PBE0		PBE		HF	
	BSa		BSb							
	HA	Δ	HA	Δ	HA	Δ	HA	Δ	HA	Δ
	Water									
ω_1	1662	-74	1627	-79	1668	-75	1632	-72	1770	-77
ω_2	3801	-147	3795	-140	3878	-145	3703	-136	4153	-137
ω_3	3917	-182	3897	-171	3999	-179	3823	-173	4270	-167
	Methane									
ω_1	1354	-44	1338	-47	1345	-43	1303	-44	1469	-46
ω_2	1576	-45	1556	-44	1575	-44	1532	-45	1685	-46
ω_3	3046	-119	3025	-115	3067	-117	2992	-123	3175	-104
ω_4	3161	-145	3126	-141	3200	-145	3119	-151	3286	-120
	Formaldehyde									
ω_1	1200	-41	1198	-39	1206	-40	1153	-40	1335	-36
ω_2	1273	-33	1262	-28	1276	-32	1232	-33	1376	-28
ω_3	1552	-47	1529	-42	1554	-46	1507	-47	1668	-42
ω_4	1848	-28	1812	-26	1881	-27	1798	-28	2029	-27
ω_5	2896	-149	2882	-146	2926	-148	2808	-156	3121	-130
ω_6	2952	-132	2937	-133	2986	-136	2850	-128	3196	-121

ure 3 is very similar to that of Figure 2 and reports the mean absolute deviation of the energies of the vibrational states with respect to fully converged values, as a function of N_{quanta}. All values reported in the figure are computed with the VCI@VSCF approach. Filled and empty symbols correspond to 3M4T and 2M4T representations of the PES, respectively. We observe that: i) all vibrational states converge as a function of the VCI truncation; ii) vibrational states characterized by an increasing number of excitation quanta (1Q, 2Q, 3Q) show a slower convergence with N_{quanta}: fundamental transitions (with 1Q) almost perfectly converge at $N_{\text{quanta}} = 4$, first overtones and two-quanta combination states (with 2Q) almost converge at $N_{\text{quanta}} = 5$ and second overtones (with 3Q) almost converge at $N_{\text{quanta}} = 6$; iii) as already discussed for fundamental transitions in Figure 2, the inclusion of three-mode terms in the PES makes the convergence generally slower, and even more so for highly excited vibrational states.

Now, we discuss the effect of the adopted basis set and exchange-correlation functional in the description of the PES on the anharmonic correction to the harmonic vibration frequencies. Both molecular and solid systems are considered. The effect of the basis set is investigated as follows: for molecular systems (water, methane and formaldehyde), a 6-31G* and a aug-cc-pvtz basis sets are used, while for solid ice-XI a 8-411G* and a POB-TZVP basis sets are used. Different methods and exchange-correlation functionals are also explored: Hartree-Fock (HF), PBE, PBE0 and B3LYP for molecules, and LDA, PBE, PBE0 and B3LYP for solids.

Table I documents the effect of the basis set and Hamiltonian on the harmonic and anharmonic vibration frequencies of three molecular systems: water, methane and formaldehyde. The computed values of the harmonic (HA) frequencies are reported, along with the corresponding anharmonic correction ($\Delta = \omega_{\text{anharm}} - \omega_{\text{harm}}$) obtained from VCI@VSCF calculations on a 3M4T representation of the PES. We see that, while the computed absolute values of the harmonic frequencies vary significantly as a function of the adopted basis set and especially of the Hamiltonian used, the anharmonic correction Δ is way less sensitive to the description of the potential. This is particularly true within the DFT but surprisingly holds also when the simple HF method is used to describe the potential. As an example, let us consider the ω_2 frequency of water: while the computed harmonic value changes from 3703 cm^{-1} of PBE to 4153 cm^{-1} of HF (a difference of 450 cm^{-1} on the absolute harmonic value), the anharmonic correction Δ is very similar in all cases, and only differs by 1 cm^{-1} between PBE and HF. Therefore, Table I has a computationally interesting implication: for these type of molecular systems (without inter-molecular interactions), while an accurate (and generally more expensive) description of the quadratic terms of the potential is needed to get accurate absolute harmonic values, the anharmonic correction can be estimated in terms of a less computationally expensive description of the higher order terms of the PES. This aspect has already been extensively discussed in the molecular literature on anharmonicity.[39–43]

The effect of different basis sets and exchange-correlation functionals on the description of the PES and therefore of the anharmonic vibrational states of the low-temperature, proton-ordered phase of solid water, ice-XI,[44–46] is shown in Table II. A subset of twelve modes is considered that have been selected so as to span the whole vibrational spectrum. Modes 1-4 correspond to molecular "translations" where the water molecules of the lattice are rigidly translating with respect to one another, modes 5-7 correspond to "librations" where the water molecules are rigidly rotating with respect to one another, modes 8-9 correspond to the "bending" of water molecules and, finally, modes 10-12 correspond to the "stretching" of water molecules.

Table II reports the computed anharmonic frequencies (as obtained with the VCI@VSCF method on a 2M4T representation of the PES) as well as the anharmonic

TABLE II. Effect of basis set and Hamiltonian on computed harmonic and anharmonic vibration frequencies (in cm^{-1}) of ice-XI. Two basis sets are used: a 8-411G* (BSa) and a POB-TZVP (BSb). Four exchange-correlation functionals of the DFT are used: LDA, PBE, PBE0 and B3LYP. The anharmonic (VCI) values of twelve selected frequencies are reported along with the anharmonic correction ($\Delta = \omega_{\rm anharm} - \omega_{\rm harm}$). The VCI@VSCF method is used on a 2M4T representation of the PES. For those frequencies that correspond to intense IR or Raman spectral features, experimental values are also given.[47,48]

	BSa								BSb		Exp.
	LDA		PBE		PBE0		B3LYP		B3LYP		
	VCI	Δ	VCI	Δ	VCI	Δ	VCI	Δ	VCI	Δ	
Translations											
ω_1	362	-11	292	-1	285	1	273	-1	270	-4	283
ω_2	447	14	315	5	299	6	281	4	281	0	283
ω_3	558	16	408	4	392	5	371	3	375	-1	-
ω_4	561	10	409	1	393	2	371	1	373	-5	-
Librations											
ω_5	1251	9	1045	-3	1028	1	993	3	986	-19	985
ω_6	1332	10	1116	4	1094	8	1045	-2	1039	-20	1020
ω_7	1535	14	1289	-1	1249	3	1196	-1	1182	-17	-
Bending											
ω_8	1454	-96	1565	-41	1624	-37	1615	-38	1608	-45	1600
ω_9	1691	-37	1690	-37	1734	-33	1716	-35	1707	-42	-
Stretching											
ω_{10}	1567	-464	2653	-111	2941	-134	2983	-128	2992	-140	-
ω_{11}	1760	-403	2718	-164	3059	-134	3100	-124	3112	-129	3087
ω_{12}	1739	-424	2710	-174	3053	-142	3093	-133	3103	-143	3087

TABLE III. Harmonic (HA) and anharmonic vibration frequencies (in cm^{-1}) for fundamental transitions, first overtones and two-quanta combination states of formaldehyde (CH_2O). Computed values (B3LYP functional with aug-cc-pVTZ basis set) are obtained by using the VSCF and VCI approaches on both a 2M4T and 3M4T representation of the PES. Experimental results are from Ref. 49. Previous results from Seidler *et al.*[50] are also reported as obtained from a VCI approach on a 4M4T representation of the PES. The quantity ΔΔ is the difference between those previously computed frequencies and our VCI ones on the 3M4T PES.

	This Study					Ref. 50		Exp.
	HA	VSCF		VCI		VCI	ΔΔ	
		2M4T	3M4T	2M4T	3M4T	4M4T		
ω_1	1198	1163	1163	1159	1159	1162	3	1167
ω_2	1262	1241	1241	1239	1234	1234	0	1249
ω_3	1529	1498	1498	1494	1487	1491	5	1500
ω_4	1812	1789	1788	1787	1786	1786	0	1746
ω_5	2882	2774	2774	2741	2736	2743	7	2782
ω_6	2937	2783	2781	2760	2804	2795	-9	2843
$2\omega_1$	2396	2334	2334	2314	2314	2320	6	2327
$2\omega_2$	2524	2489	2488	2476	2465	2464	-1	2493
$2\omega_4$	3624	3561	3559	3558	3557	3555	-2	3472
$\omega_1+\omega_3$	2727	2662	2662	2668	2646	2652	6	2656
$\omega_1+\omega_4$	3010	2946	2945	2955	2939	2941	2	2905
$\omega_2+\omega_4$	3074	3027	3026	3038	3026	3019	-7	3000
$\omega_3+\omega_4$	3341	3284	3283	3291	3265	3270	5	3238

correction Δ defined as the difference between anharmonic and harmonic values. It can be seen that, as expected, stretching modes are more anharmonic than bending modes that are in turn more anharmonic than librations and translations.

At variance with the simple molecular cases discussed above, ice-XI is characterized by a complex interplay of intra- and inter-molecular interactions, which makes its vibrational states more dependent on the description of the potential. Four different functionals are used in Table II: LDA, PBE, PBE0 and B3LYP, belonging to different classes (LDA, GGA and hybrids). Also in this case, the use of different functionals results in very different absolute values of the computed frequencies. In this respect, comparison with available experimental data[47,48] (for those modes, among the selected twelve, that correspond to intense IR or Raman spectral features) shows that hybrid functionals (either PBE0 or B3LYP) provide an excellent description of the absolute values of the computed frequencies, upon correction for anharmonicity.

From the analysis of the Δ in Table II, we see that the anharmonic corrections computed from PBE, PBE0 and B3LYP calculations, performed with the same basis set BSa, are rather consistent apart from the overestimation of the anharmonicity of stretching modes by PBE. The description of the nuclear PES and therefore of the vibrational states provided by the LDA is unsatisfactory both on absolute values and on the anharmonic correction. The effect of the adopted basis set is illustrated for the B3LYP functional and is seen to be significant, particularly so in the description of low-frequency translational and librational modes. In all cases, the use of a richer basis set produces a larger anharmonic correction to the computed harmonic frequencies.

Now, we report a comparative study to document how different descriptions of the PES (2M4T versus 3M4T representations) and different methodologies to treat the anharmonicity of the PES (VSCF versus VCI) affect computed vibrational states. To do so, we consider two simple systems (the methane and formaldehyde molecules) for which accurate reference values are available from experiments or previous calculations.

Table III reports computed harmonic and anharmonic energies of several vibrational states (fundamental transitions, first overtones and two-quanta combination states) of formaldehyde, as well as a comparison with experimental values[49] and previously computed values.[50] Our calculations are performed with the B3LYP hybrid functional and by using the aug-cc-pVTZ basis set: same conditions as in the previous theoretical investigation by Seidler *et al.* for sake of comparison and validation of our

TABLE IV. Harmonic (HA) and anharmonic vibration frequencies for fundamental transitions of methane. Experimental frequencies[51] are given in absolute value while for computed quantities, the difference Δ with respect to the experiment is given. Calculations are performed with the B3LYP hybrid functional and the 6-31G* basis set. All data are in cm^{-1}.

	Δ					Exp.
	HA	VSCF (2M4T)	VSCF (3M4T)	VCI (2M4T)	VCI (3M4T)	
ω_1	48	15	15	13	4	1306
ω_2	42	1	1	0	-3	1534
ω_3	129	68	68	22	11	2917
ω_4	142	51	51	41	-2	3019

implementation.[50] Several considerations can be made: i) for a given representation of the PES, computed VCI frequencies for fundamental transitions and first overtones are systematically smaller than computed VSCF frequencies (i.e. a more explicit account of mode-mode couplings results in a larger anharmonic correction); ii) mode-mode couplings have the opposite effect on combination states, where the use of VCI results in higher frequencies than VSCF; iii) the inclusion of three-mode terms in the PES (i.e. passing from the 2M4T to the 3M4T representation of the PES) produces almost no change in the computed VSCF frequencies while it affects more VCI computed frequencies, particularly so for ω_3, ω_5, ω_6 and combination states; iv) the quantity $\Delta\Delta$ is the difference between previously computed VCI frequencies and our VCI ones: given that the numerical evaluation of second-, third-, and fourth-order terms of the PES is different in the two implementations, the agreement on the absolute value of computed anharmonic frequencies is rather impressive, which confirms the correctness of our implementation; v) interestingly, most computed values of anharmonic frequencies compare very satisfactorily with experimental values, not just for fundamental transitions but also for overtones and combination bands.

The case of the methane molecule is documented in Table IV, where harmonic and anharmonic computed values for the frequencies of fundamental transitions are compared with experimental data.[51] For computed quantities, their difference Δ with respect to experimental values is reported. The table shows the effect of treating the anharmonicity with both the VSCF and VCI approaches and of describing the PES with both a 2M4T and a 3M4T representation. All calculations are performed with the B3LYP hybrid functional and the 6-31G* basis set. From the table, we see that the harmonic approximation (HA) overestimates the value of the four frequencies, by about 40-50 cm^{-1} for ω_1 and ω_2, and by about 130-140 cm^{-1} for ω_3 and ω_4. The VSCF method is seen to be able to account for a significant fraction of anharmonicity (Δ decreases), particularly so for the ω_2 mode, which turns out not to benefit from a more explicit account of mode-mode couplings. At the same time, the limitations of VSCF are quite evident when comparing results obtained from a 2M4T PES with those from a 3M4T PES: three-mode terms of the potential have no impact whatsoever on VSCF computed anharmonic energies. The explicit treatment of mode-mode couplings provided by VCI results in the further reduction of the Δ, particularly so for the stretching modes ω_3 and ω_4. Furthermore, the VCI approach is able to take into account three-mode terms of the PES, with a significant effect on ω_1, ω_3, and, especially, on ω_4. Finally, the agreement of the computed anharmonic frequencies (as obtained with the best methodology: VCI on a 3M4T PES) with experimental ones is rather satisfactory, with deviations generally smaller than 10 cm^{-1}. A similar result is obtained for formaldehyde in Table III, which seems to suggest that the combined use of the B3LYP hybrid functional and basis sets of triple-zeta quality provide a "lucky" cancellation of errors resulting in a good description of harmonic frequencies and thus of the absolute values of anharmonic ones.

V. CONCLUSIONS AND PERSPECTIVES

We have implemented the vibrational self-consistent field (VSCF) method and the vibrational configuration interaction (VCI) method in the public CRYSTAL program to compute anharmonic vibrational states of solids. We have reviewed the main formal aspects of the two methodologies and introduced all their relevant computational parameters. While VSCF is a mean-field approach where each vibration mode interacts with an average potential over all the other modes, VCI allows for an explicit account of mode-mode coupling.

We have discussed different strategies to effectively truncate the VCI expansion of the nuclear wavefunction. In order to allow for a more computationally efficient truncation of the VCI expansion, we have implemented a VCI@VSCF version of the VCI method where the modals used in the expansion of the vibrational wavefunction are obtained from a previous VSCF calculation on a reference vibrational state. The convergence of computed vibrational states (involving one or two quanta of excitation) with respect to the truncation of the VCI expansion has been illustrated on both molecular and solid systems.

The effect of the adopted basis sets and exchange-correlation functionals in the description of the adiabatic potential energy surface on the computed vibrational states (both at the harmonic and anharmonic level) has been documented on selected systems. Computed anharmonic values for vibrational transitions have been compared to available experimental and computational data to validate the implementation and the approach.

From a computational point of view, the bottleneck of the current implementation is represented by the memory allocation of the VCI Hamiltonian matrix. In the context

of parallel computing, a future development will be the distribution of such matrix over multiple processes so as to decrease the memory footprint of the implementation.

As a perspective, we also plan on extending the current module of the CRYSTAL program for the calculation of anharmonic vibrational states of solids to the VPT2 methodology, and to the calculation of anharmonic infrared and Raman intensities at VSCF and VCI level.

ACKNOWLEDGMENTS

A.E. and J.M. thank the University of Torino and the Compagnia di San Paolo for funding (CSTO169372). P.C. and M.R. gratefully acknowledge the GENCI (Grand Equipement National de Calcul Intensif) for computing facilities through the project number A0030810320 at TGCC/Irene (Très Grand Centre de Calcul) CEA, France.

* alessandro.erba@unito.it

[1] Born, M.; Huang, K. *Dynamical Theory of Crystal Lattices*; Clarendon Press, 1954.

[2] Maradudin, A. A.; Montroll, E. W.; Weiss, G. H. *Theory of Lattice Dynamics in The Harmonic Approximation*; Academic Press New York, 1963; Vol. 3.

[3] Baroni, S.; de Gironcoli, S.; Corso, A. D.; Giannozzi, P. Phonons and Related Crystal Properties from Density-Functional Perturbation Theory. *Rev. Mod. Phys.* **2001**, *73*, 515.

[4] Togo, A.; Tanaka, I. First Principles Phonon Calculations in Materials Science. *Scr. Mater.* **2015**, *108*, 1 – 5.

[5] Pascale, F.; Zicovich-Wilson, C. M.; Gejo, F. L.; Civalleri, B.; Orlando, R.; Dovesi, R. The calculation of the vibrational frequencies of the crystalline compounds and its implementation in the CRYSTAL code. *J. Comp. Chem.* **2004**, *25*, 888–897.

[6] Gonze, X.; Lee, C. Dynamical matrices, Born effective charges, dielectric permittivity tensors, and interatomic force constants from density-functional perturbation theory. *Phys. Rev. B* **1997**, *55*, 10355.

[7] Carbonniere, P.; Barone, V. Coriolis Couplings in Variational Computations of Vibrational Spectra Beyond the Harmonic Approximation: Implementation and Validation. *Chem. Phys. Lett.* **2004**, *392*, 365 – 371.

[8] Bowman, J. M.; Carter, S.; Huang, X. MULTIMODE: A Code to Calculate Rovibrational Energies of Polyatomic Molecules. *Int. Rev. Phys. Chem.* **2003**, *22*, 533–549.

[9] Carter, S.; Bowman, J. M. The Adiabatic Rotation Approximation for Rovibrational Energies of Many-mode Systems: Description and Tests of the Method. *J. Chem. Phys.* **1998**, *108*, 4397–4404.

[10] Erba, A.; Maul, J.; Ferrabone, M.; Carbonniére, P.; Dovesi, R.; Rérat, M. Anharmonic Vibrational States of Solids from DFT Calculations. Part I: Description of the Potential Energy Surface. *J. Chem. Theory Comput.* **2019**, submitted.

[11] Christiansen, O.; Luis, J. M. Beyond Vibrational Self-Consistent-Field Methods: Benchmark Calculations for the Fundamental Vibrations of Ethylene. *Int. J. Quantum Chem.* **2005**, *104*, 667–680.

[12] Christiansen, O. Vibrational Structure Theory: New Vibrational Wave Function Methods for Calculation of Anharmonic Vibrational Energies and Vibrational Contributions to Molecular Properties. *Phys. Chem. Chem. Phys.* **2007**, *9*, 2942–2953.

[13] Bowman, J. M. The Self-Consistent-Field Approach to Polyatomic Vibrations. *Acc. Chem. Res.* **1986**, *19*, 202–208.

[14] Gerber, R.; Ratner, M. A. Self-consistent-field methods for vibrational excitations in polyatomic systems. *Adv. Chem. Phys.* **1988**, *70*, 97–132.

[15] Rauhut, G. Efficient calculation of potential energy surfaces for the generation of vibrational wave functions. *J. Chem. Phys.* **2004**, *121*, 9313–9322.

[16] Norris, L. S.; Ratner, M. A.; Roitberg, A. E.; Gerber, R. B. Moller-Plesset perturbation theory applied to vibrational problems. *J. Chem. Phys.* **1996**, *105*, 11261–11267.

[17] Christiansen, O. Moller-Plesset perturbation theory for vibrational wave functions. *J. Chem. Phys.* **2003**, *119*, 5773–5781.

[18] Chaban, G. M.; Jung, J. O.; Gerber, R. B. Ab initio calculation of anharmonic vibrational states of polyatomic systems: Electronic structure combined with vibrational self-consistent field. *J. Chem. Phys.* **1999**, *111*, 1823–1829.

[19] Christiansen, O. A second quantization formulation of multimode dynamics. *J. Chem. Phys.* **2004**, *120*, 2140–2148.

[20] Christiansen, O. Vibrational Coupled Cluster Theory. *J. Chem. Phys.* **2004**, *120*, 2149–2159.

[21] Bowman, J. M.; Christoffel, K.; Tobin, F. Application of SCF-SI Theory to Vibrational Motion in Polyatomic Molecules. *J. Phys. Chem.* **1979**, *83*, 905–912.

[22] Zaki, K.; Gélizé-Duvignau, M.; Pouchan, C. Ab initio Cl calculations of the anharmonic force field of methyleneimine CH2NH. *J Chim. Phys. PCB* **1997**, *94*, 37–53.

[23] Carbonnière, P.; Dargelos, A.; Pouchan, C. The VCI-P Code: An Iterative Variation–Perturbation Scheme for Efficient Computations of Anharmonic Vibrational Levels and Ir Intensities of Polyatomic Molecules. *Theo. Chem. Acc.* **2010**, *125*, 543–554.

[24] Baraille, I.; Larrieu, C.; Dargelos, A.; Chaillet, M. Calculation of Non-Fundamental IR Frequencies and Intensities at the Anharmonic Level. I. The Overtone, Combination And Difference Bands of Diazomethane, H_2CN_2. *Chem. Phys.* **2001**, *273*, 91 – 101.

[25] Neff, M.; Rauhut, G. Toward Large Scale Vibrational Configuration Interaction Calculations. *J. Chem. Phys.* **2009**, *131*, 124129.

[26] Chakraborty, A.; Truhlar, D. G.; Bowman, J. M.; Carter, S. Calculation of Converged Rovibrational Energies and Partition Function for Methane Using Vibrational-Rotational Configuration Interaction. *J. Chem. Phys.* **2004**, *121*, 2071–2084.

[27] Rauhut, G. Configuration Selection as a Route Towards Efficient Vibrational Configuration Interaction Calculations. *J. Chem. Phys.* **2007**, *127*, 184109.

[28] Cassam-Chenaï, P.; Liévin, J. The VMFCI Method: A Flexible Tool for Solving the Molecular Vibration Problem.

J. Comput. Chem. **2006**, *27*, 627–640.

[29] Ribeiro, F.; Iung, C.; Leforestier, C. A Jacobi-Wilson Description Coupled to a Block-Davidson Algorithm: An Efficient Scheme to Calculate Highly Excited Vibrational Levels. *J. Chem. Phys.* **2005**, *123*, 054106.

[30] Scribano, Y.; Benoit, D. M. Iterative Active-Space Selection for Vibrational Configuration Interaction Calculations Using a Reduced-Coupling VSCF Basis. *Chem. Phys. Lett.* **2008**, *458*, 384 – 387.

[31] Dovesi, R.; Erba, A.; Orlando, R.; Zicovich-Wilson, C. M.; Civalleri, B.; Maschio, L.; Rérat, M.; Casassa, S.; Baima, J.; Salustro, S.; Kirtman, B. Quantum-Mechanical Condensed Matter Simulations with CRYSTAL. *WIREs Comput. Mol. Sci.* **2018**, *8*, e1360.

[32] Erba, A.; Baima, J.; Bush, I.; Orlando, R.; Dovesi, R. Large Scale Condensed Matter DFT Simulations: Performance and Capabilities of the CRYSTAL Code. *J. Chem. Theory Comput.* **2017**, *13*, 5019–5027.

[33] Dunning, T. H. Gaussian Basis Sets for Use in Correlated Molecular Calculations. I. The Atoms Boron Through Neon and Hydrogen. *J. Chem. Phys.* **1989**, *90*, 1007–1023.

[34] Kendall, R. A.; Dunning, T. H.; Harrison, R. J. Electron Affinities of the First-Row Atoms Revisited. Systematic Basis Sets and Wave Functions. *J. Chem. Phys.* **1992**, *96*, 6796–6806.

[35] Peintinger, M. F.; Oliveira, D. V.; Bredow, T. Consistent Gaussian Basis Sets of Triple-Zeta Valence with Polarization Quality for Solid-State Calculations. *J. Comput. Chem.* **2013**, *34*, 451–459.

[36] Becke, A. D. Density-functional thermochemistry. III. The role of exact exchange. *J. Chem. Phys.* **1993**, *98*, 5648.

[37] Perdew, J. P.; Burke, K.; Ernzerhof, M. *Phys. Rev. Lett.* **1996**, *77*, 3865.

[38] Adamo, C.; Barone, V. Toward Reliable Density Functional Methods without Adjustable Parameters: the PBE0 Model. *J. Chem. Phys.* **1999**, *110*, 6158–6170.

[39] Carbonniere, P.; Barone, V. Performances of Different Density Functionals in the Computation of Vibrational Spectra Beyond the Harmonic Approximation. *Chem. Phys. Lett.* **2004**, *399*, 226 – 229.

[40] Boese, A. D.; Martin, J. M. L. Vibrational Spectra of the Azabenzenes Revisited: Anharmonic Force Fields. *J. Phys. Chem. A* **2004**, *108*, 3085–3096.

[41] Carbonniere, P.; Lucca, T.; Pouchan, C.; Rega, N.; Barone, V. Vibrational Computations Beyond the Harmonic Approximation: Performances of the B3LYP Density Functional for Semirigid Molecules. *J. Comput. Chem.* **2005**, *26*, 384–388.

[42] Hanson-Heine, M. W. D.; George, M. W.; Besley, N. A. Investigating the Calculation of Anharmonic Vibrational Frequencies Using Force Fields Derived from Density Functional Theory. *J. Phys. Chem. A* **2012**, *116*, 4417–4425.

[43] Barnes, L.; Schindler, B.; Compagnon, I.; Allouche, A.-R. Fast and Accurate Hybrid QM//MM Approach for Computing Anharmonic Corrections to Vibrational Frequencies. *J. Mol. Model.* **2016**, *22*, 285.

[44] Erba, A.; Casassa, S.; Maschio, L.; Pisani, C. DFT and Local-MP2 periodic study of the structure and stability of two proton ordered polymorphs of ice. *J. Phys. Chem. B* **2009**, *113*, 2347.

[45] Erba, A.; Casassa, S.; Dovesi, R.; Maschio, L.; Pisani, C. Periodic density functional theory and local-MP2 study of the librational modes of Ice XI. *J. Chem. Phys.* **2009**, *130*, 074505.

[46] Pisani, C.; Maschio, L.; Casassa, S.; Halo, M.; Erba, A. A local-MP2 approach to the ab initio study of electron correlation in crystals and to the simulation of vibrational spectra: the case of Ice XI. *Theor. Chem. Acc.* **2009**, *123*, 327.

[47] Abe, K.; Shigenari, T. Raman Spectra Of Proton Ordered Phase XI of ICE I. Translational Vibrations Below 350 cm-1. *J. Chem. Phys.* **2011**, *134*, 104506.

[48] Shigenari, T.; Abe, K. Vibrational modes of hydrogens in the proton ordered phase XI of ice: Raman spectra above 400 cm-1. *J. Chem. Phys.* **2012**, *136*, 174504.

[49] Reisner, D. E.; Field, R. W.; Kinsey, J. L.; Dai, H. Stimulated Emission Spectroscopy: A Complete Set of Vibrational Constants for $\tilde{X}^1A_1$ Formaldehyde. *J. Chem. Phys.* **1984**, *80*, 5968–5978.

[50] Seidler, P.; Kongsted, J.; Christiansen, O. Calculation of Vibrational Infrared Intensities and Raman Activities Using Explicit Anharmonic Wave Functions. *J. Phys. Chem. A* **2007**, *111*, 11205–11213.

[51] Shimanouchi, T. *Tables of Molecular Vibrational Frequencies. Consolidated Volume I*; Washington, D.C. : National Bureau of Standards, 1972; pp 1–160.